

# Standard Set-Valued Young Tableaux and Product-Coproduct Prographs

Ashley Borchardt<sup>1</sup>, Maxwell Krueger<sup>2</sup>, Meghan Wren<sup>3</sup>  
Advisor: Dr. Paul Drube<sup>4</sup>

<sup>1</sup>Minnesota State University Moorhead

<sup>2</sup>Muhlenberg College

<sup>3</sup>SUNY Brockport

<sup>4</sup>Valparaiso University

VERUM 2017

Funded by NSF Grant DMS-1559912

## Abstract

Standard set-valued Young tableaux are a generalization of standard Young tableaux where cells can contain more than one integer. Unlike standard Young tableaux, there is no known method to count the number of distinct standard set-valued tableaux of arbitrary shape. In this paper, we construct bijections between standard set-valued tableaux and  $k$ -ary product-coproduct prographs, a generalization of  $k$ -ary trees where internal vertices may be interpreted as either a  $k$ -ary product or  $k$ -ary coproduct. We present a bijection between three row rectangular tableaux that have  $k - 1$  integers in each middle row cell and  $k$ -ary prographs with  $n$  products and coproducts, and then generalize our bijection to non-rectangular tableaux. We use this bijection to count the number of tableaux for small values of  $n$ . Furthermore, we investigate various intuitive operations on  $k$ -ary prographs and their corresponding standard set-valued tableaux. Finally, we define an analogue of the Schützenberger involution for standard set-valued tableaux and show it corresponds to a 180-degree rotation on  $k$ -ary prographs.

## 1 Introduction to Standard Young Tableaux

For a non-increasing integer partition  $\lambda = (\lambda_1, \dots, \lambda_m)$  of an integer  $N$ , a **Young diagram**  $Y$  of shape  $\lambda$  is a left-justified array of  $N$  cells with  $\lambda_i$  cells in the  $i^{\text{th}}$  row. Given a Young diagram of shape  $\lambda$ , a **Young tableau** of the same shape is a bijection from the set of integers  $[N] = \{1, \dots, N\}$  to the cells of  $Y$ . In order for a Young tableau to be a **standard Young tableau**, the entries in the tableau must increase left-to-right across each row and down each column. We denote the set of distinct standard Young tableaux of shape  $\lambda$  as  $S(\lambda)$ . See Figure 1 for  $S(\lambda)$  with  $\lambda = (3, 3)$ . The number of tableaux of arbitrary shape can be determined using the Hook-Length formula, given by Frame, Robinson, and Thrall [1]. For a full introduction to Young tableaux, see Fulton [2].

1	2	3
4	5	6

1	2	4
3	5	6

1	2	5
3	4	6

1	3	4
2	5	6

1	3	5
2	4	6

Figure 1: The elements of  $S(\lambda)$  for  $\lambda = (3, 3)$

We can also define two Young diagrams  $Y$  and  $Y'$ , where  $Y$  has shape  $\lambda = (\lambda_1, \dots, \lambda_m)$ ,  $Y'$  has shape  $\mu = (\mu_1, \dots, \mu_m)$ , and  $0 \leq \mu_i \leq \lambda_i$ . If  $\mu_i$  cells are removed, left-to-right, from the  $i^{\text{th}}$  row of  $Y$ , then the overall diagram becomes a **skew Young diagram**. A **skew standard Young tableau** is an assignment of positive integers to the cells of a skew diagram, where the entries increase left-to-right across each row and down each column. We denote the set of skew standard Young tableaux of shape  $\lambda$  minus  $\mu$  as  $S(\lambda/\mu)$ . See Figure 2 for  $S(\lambda/\mu)$  where  $\lambda = (3, 2)$  and  $\mu = (1, 0)$ .

	1	2
3	4	

	1	3
2	4	

	1	4
2	3	

	2	3
1	4	

	2	4
1	3	

Figure 2: The elements of  $S(\lambda/\mu)$  for  $\lambda = (3, 2)$ ,  $\mu = (1, 0)$

In our research, we primarily focus on a generalization of standard Young tableaux, called standard set-valued Young tableaux. A **standard set-valued Young tableau** of shape  $\lambda$  and **density**  $\rho = (\rho_1, \dots, \rho_n)$  is a Young tableau where every cell in the  $i^{\text{th}}$  row is assigned  $\rho_i$  distinct integers, and all integers in the cell  $(i, j)$  are smaller than every integer in the cells  $(i + 1, j)$  and  $(i, j + 1)$ . We denote the set of standard set-valued Young tableaux of shape  $\lambda$  and density  $\rho$  as  $\mathbb{S}(\lambda, \rho)$ . Figure 3 illustrates five examples of standard set-valued Young tableaux of shape  $\lambda = (3, 3)$  and density  $\rho = (2, 1)$ . For explorations into these tableaux, see Heubach, Li, and Mansour [3] and Drube [4]. A density may also be assigned to a skew Young tableau, which gives a **skew standard set-valued Young tableau**. We denote the set of all skew standard set-valued tableaux as  $\mathbb{S}(\lambda/\mu, \rho)$ .

1	2	4	5	6	7
3	8	9			

1	2	3	5	7	8
4	6	9			

1	2	3	4	5	8
6	7	9			

1	2	3	4	5	6
7	8	9			

1	2	4	5	7	8
3	6	9			

Figure 3: Five standard set-valued Young tableaux for  $\lambda = (3, 3)$  and  $\rho = (2, 1)$

Unlike standard Young tableaux, there is no known formula to count the number of distinct standard set-valued Young tableaux of arbitrary shape and density. Given this fact, our initial goal for our research was to enumerate  $\mathbb{S}(\lambda, \rho)$  for a variety of shapes and densities.

## 2 Product-Coproduct Prographs

To begin, we looked at a previous work involving standard set-valued tableaux, which used rooted  $k$ -ary trees. We then considered an existing bijection between standard Young tableaux and another combinatorial object, 2-ary product-coproduct prographs, and generalized this bijection to include standard set-valued Young tableaux and  $k$ -ary product-coproduct prographs.

## 2.1 Rooted $k$ -ary Trees

A **rooted  $k$ -ary tree** is a rooted, planar graph where every non-terminal vertex has  $k$  children. The set of distinct  $k$ -ary trees with  $n$  non-terminal nodes is denoted  $\mathcal{T}_n^k$ . It is a well-known result that these  $k$ -ary trees are counted by the  $k$ -Catalan numbers, a sequence of positive integers given by  $C_n^k = \frac{1}{(k-1)n+1} \binom{kn}{n}$ , for all integers  $k \geq 1$  and  $n \geq 0$ . This sequence is a generalization of the Catalan numbers, a famous sequence of positive integers given by  $C_n = \frac{1}{n+1} \binom{2n}{n}$  for all integers  $n \geq 0$ .

In considering different combinatorial objects counted by the  $k$ -Catalan numbers, Heubach, Li, and Mansour proved that standard set-valued tableaux of shape  $\lambda = (n, n)$  and density  $\rho = (k-1, 1)$  are counted by the  $k$ -Catalan numbers. They achieved this by constructing a bijection between  $\mathbb{S}(\lambda, \rho)$  and  $\mathcal{T}_n^k$  [3].

**Theorem 2.1** (Heubach, Li, Mansour). *Let  $\lambda = (n, n)$  and  $\rho = (k-1, 1)$ . Then,  $|\mathbb{S}(\lambda, \rho)| = |\mathcal{T}_n^k| = C_n^k$ .*

Heubach, Li, and Mansour's bijection between  $\mathbb{S}(\lambda, \rho)$  and  $\mathcal{T}_n^k$ , an example of which can be seen in Figure 4, works as follows:

1. The edges of the tree are labeled in numerical order by beginning at the root vertex and traveling around the graph, moving up and to the left, labeling edges as we come to them.
2. Integers corresponding to the right-children are placed in the bottom row.
3. Integers corresponding to the remaining-children are placed in the top row, each cell receiving  $k-1$  integers.

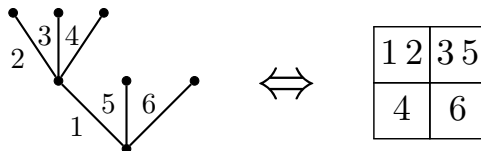


Figure 4: A 3-ary tree where  $n = 2$  and corresponding tableau

From here, we became interested in counting larger standard set-valued tableaux. This goal motivated us to focus on a generalization on these rooted  $k$ -ary trees, known as  $k$ -ary product-coproduct prographs.

## 2.2 $k$ -ary Product-Coproduct Prographs

A  **$k$ -ary product-coproduct prograph** is a rooted planar graph comprised of  $k$ -ary product and  $k$ -ary coproduct nodes. The graph is read from bottom to top to determine whether a node is a product or a coproduct node. **Product** nodes take in  $k$  edges and returns a single edge, while **coproduct** nodes take in a single edge and returns  $k$  edges. Examples of both components can be seen in Figure 5.



Figure 5: Products and coproducts for  $k = 2$  and  $k = 3$

In order for a prograph to be **closed**, the graph must begin with a single input edge and end with a single output edge. We denote the set of closed  $k$ -ary prographs with  $n$  products and  $n$  coproducts as  $PC^k(n)$ . For the full set of closed 2-ary prographs with two products and coproducts, see Figure 6.

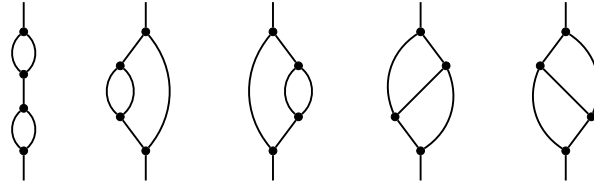


Figure 6: The elements of  $PC^2(2)$

Borie was the first to place 2-ary prographs in bijection with standard Young tableaux [5].

**Theorem 2.2** (Borie). *Let  $\lambda = (n, n, n)$ . Then,  $|S(\lambda)| = |PC^2(n)| = C_{3,n}$ .*

Here,  $C_{3,n}$  refers to  $n^{\text{th}}$  3-dimensional Catalan number. The 3-dimensional Catalan numbers are a generalization of the Catalan numbers and are given by the formula  $C_{3,n} = \frac{2(3n)!}{n!(n+1)!(n+2)!}$ , for all integers  $n \geq 0$ . Borie’s result follows directly from the Hook-Length formula. The procedure for Borie’s bijection begins with numbering the edges of the prograph using a left-ascending search. Although Borie only concerns himself with 2-ary prographs, here we define the search for  $k$ -ary prographs, as the procedure remains the same.

The left-ascending search is a numbering of the edges of a  $k$ -ary prograph, an example of which can be seen in Figure 7. The search and Borie’s procedure works as follows:

1. Number the initial input edge with 0 and proceed through the edges of the prograph staying as left as possible, labeling each unlabeled edge with an integer in numerical order. Before the output edges of a node can be labeled, all input edges of a node must be labeled first.
2. Integers corresponding to the left-coproduct children are placed in the top row of the tableau.
3. Integers corresponding to the right-coproduct children are placed in the middle row of the tableau.
4. Integers corresponding to the product children are placed in the bottom row of the tableau.

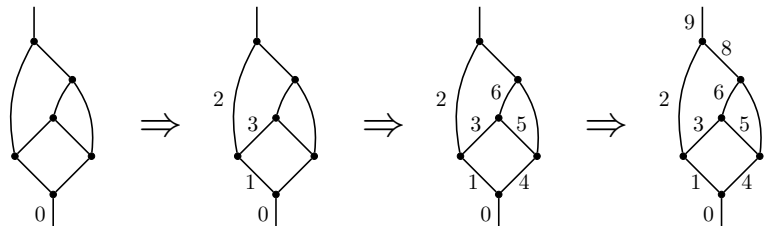


Figure 7: Example of left-ascending search on 2-ary prograph for  $n = 3$

### 3 $k$ -ary Prographs vs. Set-Valued Tableaux

In this section, we generalize Borie's bijection to standard set-valued tableaux of three rows and density  $\rho = (1, k - 1, 1)$  and  $k$ -ary prographs with  $n$  products and  $n$  coproducts. We then use our result to enumerate the number of tableaux and prographs for small  $n$ . If we can derive a formula to count standard set-valued tableaux and  $k$ -ary prographs for arbitrary  $n$  and  $k$ , this would provide a new one-parameter generalization of the 3-dimensional Catalan numbers.

**Theorem 3.1.** *Let  $k \geq 1$  be arbitrary. Then, for  $\lambda = (n, n, n)$  and  $\rho = (1, k - 1, 1)$ ,  $|\mathbb{S}(\lambda, \rho)| = |PC^k(n)|$ .*

*Proof.* Construct a bijection  $\phi : PC^k(n) \rightarrow \mathbb{S}(\lambda, \rho)$ , defined as follows:

1. Label the edges of the prograph according to the left-ascending search.
2. Place the integers corresponding to the leftmost coproduct children along the first row of the tableau from left-to-right in increasing order.
3. Place the integers corresponding to the remaining coproduct children along the middle row of the tableau from left-to-right in increasing order, each box receiving  $k - 1$  integers.
4. Place the integers corresponding to the product children along the third row of the tableau from left-to-right in increasing order.

For each leftmost coproduct child, there are always  $k - 1$  other coproduct children, so the middle row receiving  $k - 1$  integers is clearly well-defined. Moreover, due to the nature of our left-ascending search, leftmost coproduct children will always be numbered before non-leftmost coproduct children. When the  $n^{\text{th}}$  product is placed there will be  $n * k$  existing labeled coproduct edge with  $k * (n - 1)$  of those edges being inputs to previous products. This fact means there will be an additional labeled output for each product placed before the  $n^{\text{th}}$  product output is labeled. Thus, the resulting tableau will always be column standard. Due to the nature of the left-ascending search, edges of a similar type are numbered in increasing order and mapped to tableaux in the same order. Therefore, the resulting tableau will also be row standard.

The procedure for  $\phi^{-1}$  works as follows:

1. Place an initial input edge, number as 0.
2. In numerical order, consider the next integer in the tableau, which becomes the active integer.
  - (a) If the active integer is in the top row, place a coproduct on the active edge and number the leftmost child with the active integer.
  - (b) If the active integer is in the middle row, number the next unlabelled coproduct child in the existing prograph according to the left-ascending search.
  - (c) If the active integer is in the bottom row, close the active edge and  $k - 1$  left-adjacent edges into a product and the number product child with the active integer.

In performing the inverse map, there are two potential problems: either there will not be enough unlabeled edges for an active entry in the middle row, or there will not be enough labeled edges to close into a product for an active entry in the bottom row.

For the middle row, consider the active integer located in the  $i^{th}$  box of the middle row. Let  $x$  denote the active integer. Notice that, in order to have reached  $x$ ,  $i$  coproducts must have been placed. Thus, there are at least  $i * (k - 1)$  non-leftmost edges available to be labeled, and  $x$  is at most the  $i * (k - 1)^{th}$  integer needing a non-leftmost edge.

For the bottom row, consider the entry in the  $i^{th}$  box of the bottom row. To have reached this box, there must have been  $i$  coproducts placed in the prograph, contributing  $k$  already-labeled inputs each. There must also be  $i - 1$  products already placed in the prograph, consolidating  $(i - 1) * k$  inputs into  $i - 1$  outputs. Moreover, any of these  $(i - 1)$  outputs could then become coproduct inputs. Thus, the total available inputs for the  $i^{th}$  product is at least

$$i * k - (i - 1) * k + (i - 1) - (i - 1) = k$$

Therefore, there are always at least  $k$  labeled edges to close into the  $i^{th}$  product.

The two possible problems which would make  $\phi^{-1}$  not well-defined are not possible because of the row and column standardness, and thus,  $\phi^{-1}$  is well-defined. As  $\phi$  and  $\phi^{-1}$  are both well-defined, and clearly inverses of each other, the bijection between  $PC^k(n)$  and  $\mathbb{S}(\lambda, \rho)$  holds, and therefore,  $|\mathbb{S}(\lambda, \rho)| = |PC^k(n)|$ .  $\square$

An example of our generalized bijection as illustrated in the proof of Theorem 3.1 can be seen in Figure 8.

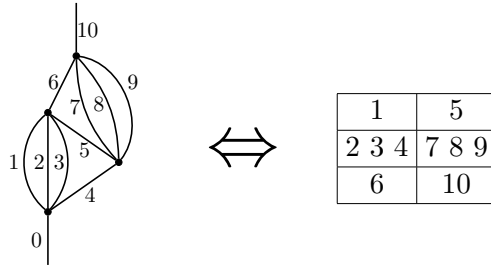


Figure 8: Example of our bijection for  $n = 2$  and  $k = 4$

### 3.1 Enumerating Standard Set-Valued Young Tableaux of Shape $\lambda = (n, n, n)$

Now that we had proven  $|\mathbb{S}(\lambda, \rho)| = |PC^k(n)|$ , we proceed to calculate the cardinality of these sets for small values of  $n$ . We begin by presenting closed-formulas for the cases of  $n = 2$ ,  $n = 3$ , and  $n = 4$ . For the  $n = 2$  case, we prove this directly. For the two larger cases, we decompose the larger shapes of tableaux into the sum of smaller shapes. Along with rigorous proofs, we are able to compare our results with the experimental values in Figure 9, which were computed using Java code written by Benjamin Levandowski of Valparaiso University.

$k \setminus n$	1	2	3	4	5	6
1	<b>1</b>	<b>2</b>	<b>5</b>	<b>14</b>	<b>42</b>	<b>132</b>
2	<b>1</b>	<b>5</b>	<b>42</b>	<b>462</b>	<b>6006</b>	<b>87516</b>
3	<b>1</b>	<b>10</b>	<b>190</b>	<b>4925</b>	153415	5396601
4	<b>1</b>	<b>17</b>	<b>581</b>	<b>27461</b>	1566018	100950800
5	<b>1</b>	<b>26</b>	<b>1401</b>	<b>105026</b>	9511451	<i>Unknown</i>

Figure 9: Cardinality of  $PC^k(n)$  and  $\mathbb{S}(\lambda, \rho)$   
Note: Numbers in bold are proven values  
(*Java Code Courtesy of Benjamin Levandowski*)

In order to directly prove the  $n = 2$  case, we must first consider the following lemma, whose proof is straight-forward and left to the reader.

**Lemma 3.2.** *Define the set  $S = [2n - 1] = \{1, \dots, 2n - 1\}$ , for arbitrary integer  $n \geq 2$ . Let  $S_1, S_2$  be pairwise disjoint subsets of  $S$ , such that  $|S_1| = n, |S_2| = n - 1$  and all elements in  $S_1$  are consecutive. Then, the number of distinct ways  $S$  can be partitioned into  $S_1 \cup S_2$  is  $n$ .*

**Theorem 3.3.** *Let  $\lambda = (2, 2, 2)$  and  $\rho = (1, k - 1, 1)$  for arbitrary  $k \geq 1$ . Then,*

$$|\mathbb{S}(\lambda, \rho)| = |PC^k(2)| = k^2 + 1.$$

*Proof.* Let  $k \in \mathbb{N}$  be arbitrary. Note, every  $P \in PC^k(2)$  must begin with a single input, followed by a  $k$ -ary coproduct. Then, all of the  $k$  outputs of this coproduct must either be inputs to a  $k$ -ary product, or one of these outputs will become an input for the second coproduct. This partitions the construction of all  $P \in PC^k(2)$  into two disjoint cases.

**Case 1:** Consider all  $P \in PC^k(2)$  beginning a  $k$ -ary product after the initial coproduct. This first product will return a single output, which then must go into the second coproduct, which then returns  $k$  outputs. The final product receives these  $k$  outputs and returns a single output, which closes the graph. Given this order of construction, there is only one prograph of this form.

**Case 2:** Consider all  $P \in PC^k(2)$  beginning with a  $k$ -ary coproduct after the initial coproduct. There are  $k$  edges that could become the input for the second coproduct. Once the final coproduct is placed, the first product must be placed. After the final coproduct is placed, there are  $2k - 1$  potential inputs for the first product. A product must receive  $k$  inputs, and to avoid the crossing of edges, these  $k$  inputs must be adjacent. Otherwise, this product would close around an unused edge, and this edge would have to cross the first product's inputs in order for the prograph to be closed. Out of these  $2k - 1$  outputs, there are  $k$  different ways to choose  $k$  adjacent inputs for the first product, by Lemma 3.2. This first product returns a single output, so the final product closes the prograph by receiving this single product output and the remaining  $k - 1$  coproduct outputs. Therefore, for each of the  $k$  choices for the second coproduct, there are  $k$  ways to place the first product, meaning that the total number of  $P \in PC^k(2)$  that begin with two consecutive coproducts is  $k^2$ .

Cases 1 and 2 are clearly distinct, and thus, the order of  $PC^k(2)$  is  $k^2 + 1$ . Given our bijection,  $|\mathbb{S}(\lambda, \rho)| = |PC^k(2)|$ , for  $\lambda = (2, 2, 2)$  and  $\rho = (1, k - 1, 1)$ .  $\square$

The argument used to prove the  $n = 2$  case is inconvenient for larger cases, as there is an increased number of ways to construct a prograph with  $n \geq 3$  products and coproducts. Therefore, to prove larger cases, we need to deconstruct the corresponding shapes of standard set-valued tableaux into the sum of smaller shapes. In the following proof for the  $n = 3$  case, the tableau shapes correspond to the number of standard set-valued tableaux of the shapes shown.

**Theorem 3.4.** *Let  $\lambda = (3, 3, 3)$  and  $\rho = (1, k - 1, 1)$  for arbitrary  $k \geq 1$ . Then,*

$$|\mathbb{S}(\lambda, \rho)| = |PC^k(3)| = \frac{9k^4 - 2k^3 + 9k^2}{4} + 1.$$

*Proof.* For any integer  $k \geq 1$ , let  $\lambda = (3, 3, 3)$  and  $\rho = (1, k - 1, 1)$ . Given that the largest integer in any tableaux in  $\mathbb{S}(\lambda, \rho)$  must appear in the rightmost bottom box, we can remove this box and not change the order of the set. Then, take an arbitrary tableau in  $\mathbb{S}((3, 3, 2), \rho)$  and consider the integers  $a$ ,  $b$ , and  $c_1$  in the boxes

		$c_1$
$a$	$b$	

Here,  $c_1$  is the smallest of the  $k - 1$  integers  $c_1, \dots, c_{k-1}$  at position  $(i, j) = (2, 3)$ . We proceed by decomposing tableaux of this shape into smaller shapes depending on where  $a, b$  fall within  $c_1 < \dots < c_{k-1}$ . In each case, we remove the cell at position  $(i, j) = (2, 3)$  and any other cell containing an integer larger than  $c_1$ .

**Case 1:** Assume  $a < b < c_1$ . In this case, the largest  $k - 1$  integers are all in box  $(i, j) = (2, 3)$ , and therefore, we can remove this box. After removal, the next largest integer must either be in boxes  $(3, 2)$  or  $(1, 3)$ , which both have a density of 1. Therefore,

$$\begin{array}{|c|c|c|} \hline & & \\ \hline & & \\ \hline & & \\ \hline \end{array} = \begin{array}{|c|c|} \hline & \\ \hline & \\ \hline & \\ \hline \end{array} + \begin{array}{|c|c|c|} \hline & & \\ \hline & & \\ \hline & & \\ \hline & & \\ \hline \end{array}$$

The diagrams shown represent the cardinality of the sets of tableaux of given shape and density  $\rho$ . Note that the order of the set  $\mathbb{S}((2, 2, 2), \rho)$  is given by  $k^2 + 1$ , by Theorem 3.3.

**Case 2:** Assume  $a < c_1 < b$ . In this case,  $b$  can be anywhere between  $c_1 < \dots < c_{k-1}$  or  $c_{k-1} < b$ ; thus, there are  $k - 1$  spots for  $b$ . Therefore, for each tableaux with boxes  $(2, 3)$  and  $(3, 2)$  removed, there are  $k - 1$  ways to return these boxes. Thus, the number of original tableaux where this inequalities holds can be decomposed into

$$(k - 1) * \begin{array}{|c|c|c|} \hline & & \\ \hline & & \\ \hline & & \\ \hline & & \\ \hline \end{array}$$



**Case 3:** Assume  $c_1 < a < b$ . In this case,  $a < b$  can be anywhere between  $c_1 < \dots < c_{k-1}$ ,  $a < c_{k-1} < b$ , or  $c_{k-1} < a < b$ . Therefore, there are  $k$  spots for these 2 integers to be placed, or  $\binom{k}{2}$ . Once these boxes are removed, we can add in the next  $k - 1$  integers to a new box in the bottom-right corner. Doing this will not change the number of these tableaux, and  $|\mathbb{S}((3, 3), \rho)|$  is known to be  $C_3^k$  [3]. Therefore, we can decompose this subset of tableaux into

$$\binom{k}{2} * \begin{array}{|c|c|c|} \hline \square & \square & \square \\ \hline \square & \square & \square \\ \hline \square & \square & \square \\ \hline \end{array} = \binom{k}{2} * C_3^k = \binom{k}{2} * \frac{1}{3k-2} \binom{3k}{3}$$

Now, the original  $3 \times 3$  tableau shape has been decomposed into

$$\begin{array}{|c|c|c|} \hline \square & \square & \square \\ \hline \square & \square & \square \\ \hline \square & \square & \square \\ \hline \end{array} = (k^2 + 1) + \begin{array}{|c|c|c|} \hline \square & \square & \square \\ \hline \square & \square & \square \\ \hline \square & \square & \square \\ \hline \end{array} + (k-1) * \begin{array}{|c|c|c|} \hline \square & \square & \square \\ \hline \square & \square & \square \\ \hline \square & \square & \square \\ \hline \end{array} + \binom{k}{2} * \frac{1}{3k-2} \binom{3k}{3}$$

Consider the tableaux of shape  $\lambda = (3, 2, 1)$ , for which we define the three possible largest integers as  $a, b, c_1$ , which are contained in the boxes

$$\begin{array}{|c|c|c|} \hline \square & \square & a \\ \hline \square & c_1 & \square \\ \hline b & \square & \square \\ \hline \end{array}$$

We split these tableaux into the five cases:

- 1)  $a, b < c_1$ , 2)  $a < c_1 < b$ , 3)  $b < c_1 < a$ , 4)  $c_1 < a < b$ , 5)  $c_1 < b < a$

The coefficients that correspond to the inequalities are the same as above, and so tableaux of this shape can be decomposed into

$$\begin{array}{|c|c|c|c|} \hline \square & \square & \square & \square \\ \hline \square & \square & \square & \square \\ \hline \square & \square & \square & \square \\ \hline \end{array} + (k-1) * \begin{array}{|c|c|c|c|} \hline \square & \square & \square & \square \\ \hline \square & \square & \square & \square \\ \hline \square & \square & \square & \square \\ \hline \end{array} + (k-1) * \begin{array}{|c|c|c|} \hline \square & \square & \square \\ \hline \square & \square & \square \\ \hline \square & \square & \square \\ \hline \end{array} + 2 \binom{k}{2} * \begin{array}{|c|c|} \hline \square & \square \\ \hline \square & \square \\ \hline \end{array}$$

The tableaux of these shapes are simple to count with binomial coefficients, and therefore

$$\begin{array}{|c|c|c|c|} \hline \square & \square & \square & \square \\ \hline \square & \square & \square & \square \\ \hline \square & \square & \square & \square \\ \hline \end{array} = \binom{k+2}{2} + (k-1) * \binom{k+1}{2} + (k-1) * (k+1) + 2 \binom{k}{2} * k$$

$$= \frac{3k^3 + k^2 + 2k}{2}.$$

From here, we can substitute this expression into

$$(k^2 + 1) + \frac{3k^3 + k^2 + 2k}{2} + (k-1) * \frac{3k^3 + k^2 + 2k}{2} + \binom{k}{2} * \frac{1}{3k-2} \binom{3k}{3}$$

$$= \frac{9k^4 - 2k^3 + 9k^2}{4} + 1.$$

□

The proof for the  $n = 4$  case is constructed in the same way as the proof for Theorem 3.4, with an increased number of cases. The expression we derived to count this case matches the values in column 4 of Figure 9, and therefore the proof is omitted.

**Theorem 3.5.** *Let  $\lambda = (4, 4, 4)$  and  $\rho = (1, k - 1, 1)$  for arbitrary  $k \geq 1$ . Then,*

$$|\mathbb{S}(\lambda, \rho)| = |PC^k(4)| = \frac{256k^6 - 114k^5 + 217k^4 - 12k^3 + 121k^2}{36} + 1.$$

Notice, the three expressions for  $n = 2$ ,  $n = 3$ ,  $n = 4$  have similar features. The denominator of the polynomials seems to be given by  $((n - 1)!)^2$ , and the initial coefficient appears to be given by  $n^{2n-4}$ . The degree of each polynomial also seems to be given by  $2n - 2$ , and each expression has no  $k^1$  term. The addition of 1 at the end of each expression corresponds to the singular case of constructing a prograph by placing a coproduct, immediately followed by a product, and repeating, as seen in the proof of Theorem 3.3. These patterns may make the problem of deriving a closed-formula for arbitrary  $n$  more tractable. However, we were unable to find such a formula for arbitrary  $n$  during our research.

However, given the experimental data for the  $n = 5$  case and the patterns we found in each proven formula, we are able to use linear regression to derive a possible expression to count five column tableaux. We assume the denominator would have the form  $((5 - 1)!)^2 = 24^2$ , and the leading coefficient would be  $5^{2*5-4} = 5^6$ . Therefore, we conjecture that the  $n = 5$  polynomial would be of the form

$$|PC^k(5)| = \frac{15625k^8 + ak^7 + bk^6 + ck^5 + dk^4 + ek^3 + fk^2}{576} + 1.$$

The experimental data in Figure 9 gives us the number of five column tableaux for  $k \in [1, 6]$ . Thus, we define a vector  $\vec{x} = (a, b, c, d, e, f)$ , for the unknown coefficients, and construct a matrix  $A$  by plugging in  $1 \leq k \leq 6$  into the above expression. Then, for each  $k$  value, we set the above expression equal to  $|PC^k(5)|$ , and solve for  $ak^7 + \dots + fk^2$ , placing the final values in a vector  $\vec{b}$ . Finally, we solve  $A * \vec{x} = \vec{b}$  for  $\vec{x}$ . If our hypothesis about the patterns is incorrect, this process may not yield the correct expression. However, the expression fits our data table, appears to return only integer values for  $k > 6$ , and shares the alternating positive and negative coefficients with the proven expressions.

**Conjecture 3.6.** *Let  $\lambda = (5, 5, 5)$  and  $\rho = (1, k - 1, 1)$  for arbitrary  $k \geq 1$ . Then,*

$$|\mathbb{S}(\lambda, \rho)| = |PC^k(5)| = \frac{15625k^8 - 10092k^7 + 10258k^6 - 72k^5 + 5473k^4 - 204k^3 + 2628k^2}{576} + 1.$$

### 3.2 Non-Closed $k$ -ary Prographs

To further generalize our initial bijection, we now consider prographs that are not closed. To do this, we allow the prographs to have multiple initial inputs, multiple terminal outputs, or both. Here we denote the set of non-closed  $k$ -ary prographs with  $n$  coproducts,  $m$  products, and  $x$  initial inputs as  $PC_x^k(n, m)$ . The bijection involving these non-closed prographs and standard set-valued tableaux will be largely equivalent to our previously defined bijection. Before giving our bijection, we establish a basic result giving the number of outgoing edges  $y$  in a non-closed  $k$ -ary prograph as a function of  $n$ ,  $m$ ,  $k$ , and  $x$ .

**Proposition 3.7.** *For a non-closed  $k$ -ary prograph with  $n$  coproducts,  $m$  products, and  $x$  initial inputs, the number of output edges is  $y = (n - m) * (k - 1) + x$ . In particular,  $y \equiv x \pmod{k - 1}$ .*

*Proof.* Let  $P$  be a  $k$ -ary prograph with  $n$  coproducts and  $m$  products. Assume  $P$  has  $x$  inputs. Observe, each coproduct contributes  $k$  edges to  $P$  and utilizes one edge as an input. Thus,  $n$  coproducts contribute

$n * (k - 1)$  edges to  $P$ . Additionally, each product utilizes  $k$  edges as inputs and contributes one edge. Thus,  $m$  products contribute  $-m * k + 1$  free edges to  $P$ . Moreover, each input edge contributes an edge within  $P$ , so  $x$  inputs contribute  $x$  edges. Hence, there are  $n * k - n - m * k + m + x$  edges in  $P$ . So

$$\begin{aligned} n * k - n - m * k + m + x &= n * (k - 1) - m * (k - 1) + x \\ &= (n - m) * (k - 1) + x. \end{aligned}$$

So,  $(n - m) * (k - 1) + x \equiv x \pmod{k - 1}$ . Note  $(n - m) * (k - 1) + x$  is the number of outputs of  $P$ , call this  $y$ . Therefore,  $y \equiv x \pmod{k - 1}$ .  $\square$

While Proposition 3.7 gives insight into the number of output edges of a non-closed  $k$ -ary prograph, we need to restrict our attention to the case of  $x \equiv 1 \pmod{k - 1}$  in order to extend our bijection to these prographs.

**Theorem 3.8.** *If  $x \equiv 1 \pmod{k - 1}$ , then  $|PC_x^k(n, m)| = |\mathbb{S}(\lambda/\mu, \rho)|$  where  $\lambda = (n + \frac{x-1}{k-1}, n + \frac{x-1}{k-1}, m)$  and  $\mu = (\frac{x-1}{k-1}, 0, 0)$ , with  $\rho = (1, k - 1, 1)$ .*

In order to prove Theorem 3.8, we must first define a specific construction of a prograph. For each non-closed prograph  $P \in PC_x^k(n, m)$ , there exists a corresponding closed prograph  $j(P)$ , called the **justified prograph** of  $P$ , where  $P$  has been closed in such a way that the  $k$  leftmost initial inputs in  $P$  are closed recursively into a coproduct until a single input edge remains. Then, the  $k$  rightmost output edges are closed recursively into a product until a single output edge remains. An example of this closing procedure can be seen in Figure 10.

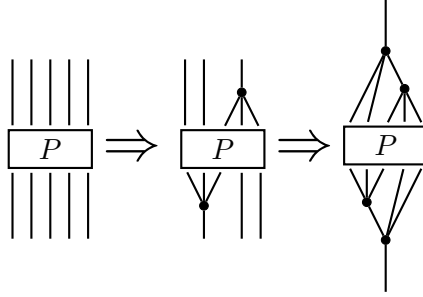
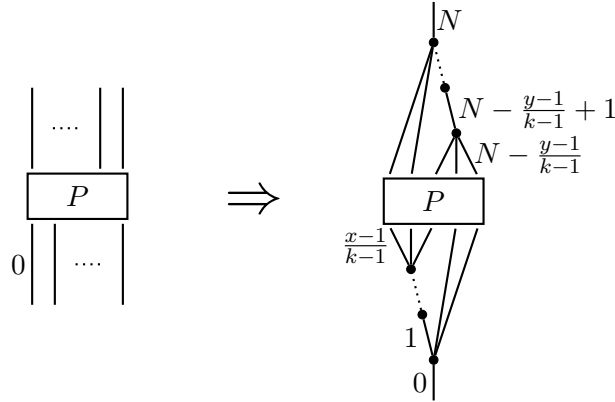


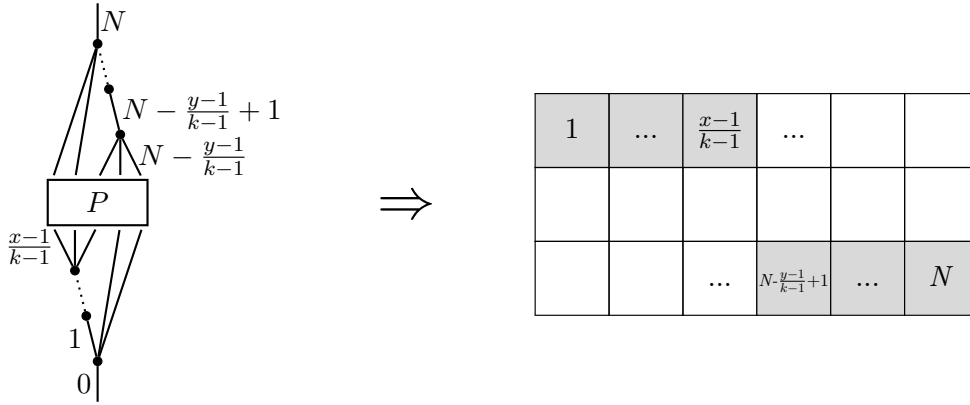
Figure 10: Closing a non-closed prograph into a justified prograph

*Proof of Theorem 3.8.* Take an arbitrary non-closed prograph  $P \in PC_x^k(n, m)$ . We know from Proposition 3.7 that  $y = (k - 1) * (n - m) + x$ . Furthermore, this expression tells us that the number of coproducts  $n$  in  $P$  is given by  $n = m + \frac{y-x}{k-1}$ . We proceed by constructing a bijection between  $PC_x^k(n, m)$  and the set of justified prographs. In order to justify  $P$ , we need to add enough coproducts on the bottom and products on the top of  $P$  to ensure that  $j(P)$  has the same number of products and coproducts. Using the expression from Proposition 3.7, we find that  $n + \frac{x-1}{k-1} = m + \frac{y-1}{k-1}$ . Therefore, we must add  $\frac{x-1}{k-1}$  coproducts to the bottom and  $\frac{y-1}{k-1}$  products to the top of  $P$ , in the way described by the definition of a justified prograph. Therefore,  $j(P) \in PC^k(n + \frac{x-1}{k-1})$ . In order for  $\frac{x-1}{k-1}$  and  $\frac{y-1}{k-1}$  to be integer values,  $k - 1$  must divide  $x - 1$  and  $y - 1$ , or  $x, y$  must be equivalent to  $1 \pmod{k - 1}$ . This justification process can be

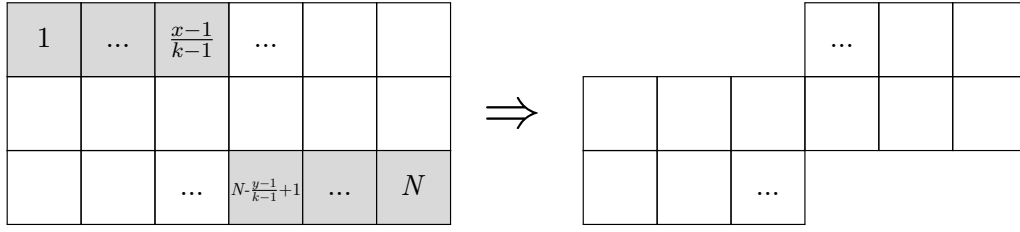
seen below for  $x = 5$ ,  $y = 5$ , and  $k = 3$ . Although the prograph in the example has an equal number of input and output edges, this need not be true.



Using our bijection  $\phi$ , we map  $j(P)$  to a standard set-valued tableau of shape  $\lambda = (n + \frac{x-1}{k-1}, n + \frac{x-1}{k-1}, n + \frac{x-1}{k-1})$  and density  $\rho = (1, k - 1, 1)$ . Given the nature of the left-ascending search, the left-coproduct children corresponding to the added  $\frac{x-1}{k-1}$  coproducts will all be labeled first. Similarly, the product children corresponding to the added  $\frac{y-1}{k-1}$  products will all be labeled last. Therefore, the top-left  $\frac{x-1}{k-1}$  boxes will contain the smallest  $\frac{x-1}{k-1}$  integers, and the bottom-right  $\frac{y-1}{k-1}$  boxes will contain the  $\frac{y-1}{k-1}$  largest integers. We show a general example of the smallest  $\frac{x-1}{k-1}$  integers in the top leftmost cells and the largest  $\frac{y-1}{k-1}$  integers in the bottom rightmost cells.



As these top-row and bottom-row boxes contain the smallest and largest integers, respectively, and have a density of one, we can remove  $\frac{x-1}{k-1}$  boxes from the top-left and  $\frac{y-1}{k-1}$  from the bottom-right and keep the resulting tableau row and column standard. We remove the top boxes from left-to-right, so if  $P$  has more than one input, removing the corresponding boxes creates a standard skew set-valued tableau. If  $P$  has more than one output, then removing the bottom boxes from right-to-left creates a non-rectangular tableau. Because the  $x - 1$  right-most input edges in  $P$  will be placed in the middle row of the corresponding tableau, the number of boxes in the middle row of the rectangular tableau does not change in the new tableau. An example of the tableau corresponding to  $P$  is shown below.



Removing these boxes creates a bijection between the subset of standard set-valued tableaux  $\mathbb{S}(\lambda, \rho)$  that correspond to justified prograhs, and the set of standard skew set-valued tableaux of shape  $\lambda = (n + \frac{x-1}{k-1}, n + \frac{x-1}{k-1}, m)$ ,  $\mu = (\frac{x-1}{k-1}, 0, 0)$  and density  $\rho = (1, k - 1, 1)$ . Given the above bijection from non-closed prograhs to justified prograhs, any non-closed prograh in  $PC_x^k(n, m)$  will map to a standard skew set-valued tableaux of shape and density described above.  $\square$

See Figure 11 for two examples which illustrate the bijection described above. The first example depicts a  $k$ -ary prograh with a single input and five outputs, and the second example depicts a  $k$ -ary prograh with three inputs and three outputs. Observe, under the bijection from Theorem 3.8, the non-leftmost input edges always appear in the middle row of the corresponding tableaux.

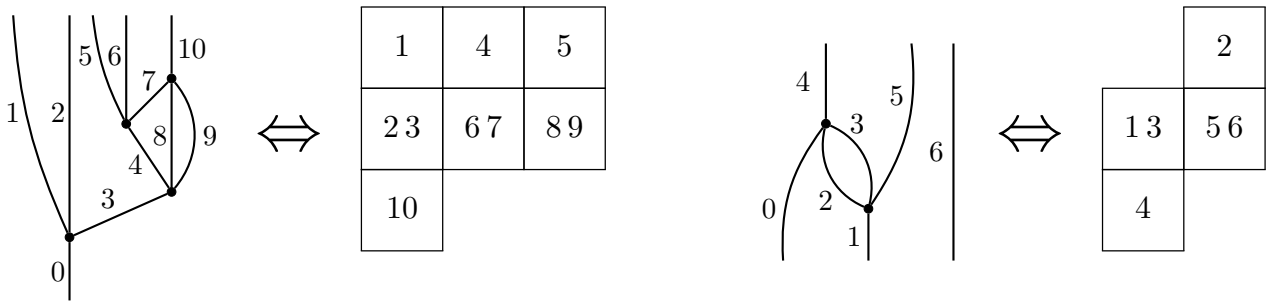


Figure 11: Non-closed prograhs and associated tableaux

## 4 Operations on $k$ -ary Prograhs and Standard Set-Valued Tableaux

After establishing our bijection between closed and non-closed  $k$ -ary prograhs and their associated standard set-valued tableaux, we begin to explore different applications of these results. Specifically, we've defined operations we can perform on  $k$ -ary prograhs and investigate the effect of those operations on the associated standard set-valued tableaux.

### 4.1 The Schützenberger Involution

The first operation we examine is the Schützenberger involution. An involution is a function that when performed twice is equivalent to the identity map. The Schützenberger involution was originally defined for standard Young tableaux. This involution works in the following manner: take  $T \in S(\lambda)$  where  $\lambda \vdash N$ , renumber the entries of  $T$  according to  $a \mapsto N - a + 1$ , and finally rotate the resulting tableau by 180-degrees. We generalize the Schützenberger involution to standard set-valued tableaux of rectangular shape  $\lambda$ , which functions equivalently. If we let  $f : \mathbb{S}(\lambda, \rho) \rightarrow \mathbb{S}(\lambda, \rho')$  denote the Schützenberger involution

on a standard set-valued Young tableau, then  $f(T)$  is defined by reversing the alphabet on  $T \in \mathbb{S}(\lambda, \rho)$  and rotating by 180-degrees. Observe that the density of the tableau may change after the involution, if the density of the original tableau is not symmetric. See Figure 12 for an illustration of the Schützenberger involution on a standard set-valued tableau.

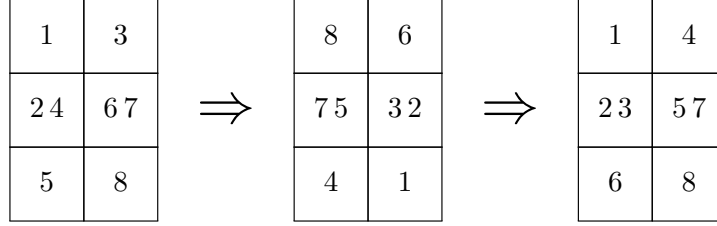


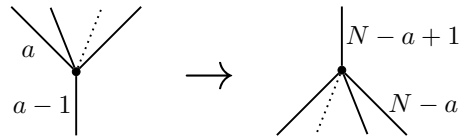
Figure 12: The Schützenberger involution on a standard set-valued tableau for  $n = 2, k = 3$

With our generalized Schützenberger involution, we want to define an equivalent operation on  $k$ -ary prographs. Borie observes that a rotation of 180-degrees is an involution when applied to 2-ary prographs [5]. We observe that this rotation is also an involution for  $k$ -ary prographs with any arbitrary value of  $k$ , so we define  $r : PC^k(n) \rightarrow PC^k(n)$  to be a 180-degree rotation on a closed  $k$ -ary prograph. Furthermore, we show that the Schützenberger involution and  $r$  are equivalent operations.

**Theorem 4.1.** *Take  $T \in \mathbb{S}(\lambda, \rho)$  for  $\lambda = (n, n, n)$  and density  $\rho = (1, k - 1, 1)$ . Then,  $\phi \circ r(T) = f \circ \phi(T)$ .*

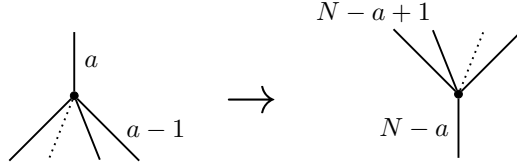
*Proof.* Take an arbitrary  $k$ -ary prograph  $p \in PC^k(n)$ . The edges in  $p$  are numbered according to the left-ascending search. For an arbitrary integer  $a \in [N]$ , the edge in  $p$  that is labeled  $a$  by the search will be re-labeled in  $r(p)$  as  $N - a$ . Considering  $\phi(p)$ , the Schützenberger involution will map  $a$  to  $N - a + 1$ . If  $a$  was originally in the top row of the tableau, the Schützenberger involution will then map  $N - a + 1$  to the bottom row, and vice versa. Once the top and bottom rows of the tableau are both filled, there is only one way to assign integers to the middle row, given row and column standardness. Therefore, we need only consider the cases where  $a$  labels a left coproduct output and where  $a$  labels a product output.

**Case 1:** Consider the case where  $a$  labels a left-coproduct output. Because of the nature of the left-ascending search, the left-coproduct edge in  $p$  and its equivalent edge in  $r(p)$  are labeled as follows:



This diagram shows that an arbitrary left-coproduct edge in  $p$  will be followed by a product output in  $r(p)$ . In  $\phi(p)$ , this left-coproduct label  $a$  appears in the top row; under  $f$ , the label becomes  $N - a + 1$  and is moved to the bottom row, and therefore will correspond to a product output. We see here that, if  $a$  originally labeled a left-coproduct in  $p$ ,  $N - a + 1$  must correspond to a product output in  $r(p)$ , and will therefore be placed in the bottom row of  $\phi(r(p))$ .

**Case 2:** Consider the case where  $a$  labels a product output. Given the nature of the left-ascending search, the product edge in  $p$  and its equivalent edge in  $r(p)$  are labeled as follows:



This diagram shows that an arbitrary product output in  $p$  will be followed by a left-coproduct output in  $r(p)$ . In  $\phi(p)$ , the label  $a$  of the product output will appear in the bottom row, and under  $f$ ,  $a$  will be mapped to  $N-a+1$  and be moved to the top row, and therefore will correspond to a left-coproduct output. We see here that, if  $a$  originally labeled a product output,  $N-a+1$  in  $r(p)$  must always correspond to a left-coproduct output, and will therefore be placed in the top row of  $\phi(r(p))$ .

Given these two cases, we see that  $r$  and  $f$  are equivalent operations on prographs and tableaux, respectively. Placing the integers in the top and bottom rows forces a single ordering of the middle row integers, so the two cases described above are sufficient.  $\square$

The relationship between  $f$  and  $r$  as illustrated in the proof of Theorem 4.1 is shown in Figure 13.

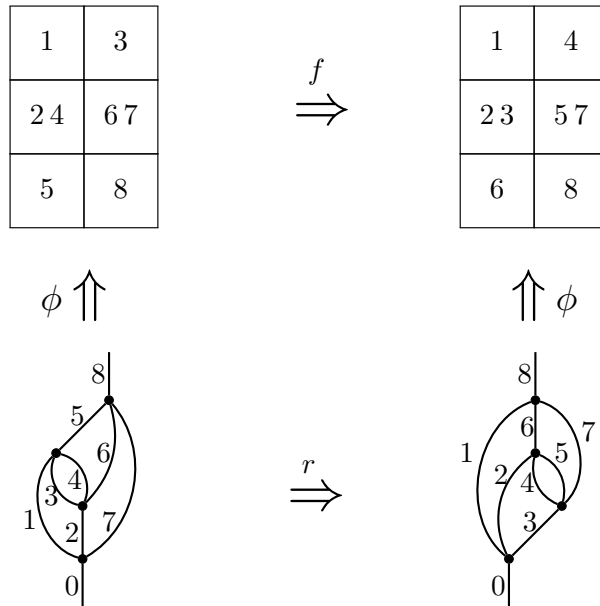


Figure 13: Relationship between the Schützenberger involution and  $r$

## 4.2 Composition

In addition to generalizing  $f$  and  $r$  for arbitrary  $k \geq 1$  and establishing an equivalence between these two functions, we also carefully examine two intuitive operations on  $k$ -ary prographs and their associated tableaux. The first of these two operations we define is the composition of two  $k$ -ary prographs. The **composition** of prographs  $P_1, P_2$ , where  $P_i \in PC^k(n_i)$ , is denoted  $P_2 \circ P_1$  and lies in  $PC^k(n_1 + n_2)$ . The composition  $P_2 \circ P_1$  replaces the initial input edge of  $P_2$  with the terminal output edge of  $P_1$  such that the second prograph is effectively stacked on top of the first. See the left half of Figure 14 for an illustration

of this operation. What we are most interested in is how the individual tableaux  $\phi(P_1)$  and  $\phi(P_2)$  appear in the tableau  $\phi(P_2 \circ P_1)$  associated with their composition. We observed the following pattern stated in Theorem 4.2 and illustrated in Figure 14.

**Theorem 4.2.** *Take  $P_1 \in PC^k(n_1)$  and  $P_2 \in PC^k(n_2)$  and let  $T_1 = \phi(P_1)$ ,  $T_2 = \phi(P_2)$ . Then  $\phi(P_1 \circ P_2) \in \mathbb{S}(\lambda, \rho)$  with  $\lambda = (n_1 + n_2, n_1 + n_2, n_1 + n_2)$ , where the first  $n_1$  columns will correspond to  $T_1$  and the final  $n_2$  columns will correspond to  $T_2$ , scaled-up.*

*Proof.* Let  $P_1$  and  $P_2$  be arbitrary prographs. Consider  $P_2 \circ P_1$ . Recall that when performing the left-ascending search, all input edges to a product must be labeled before the output edge can be labeled. Observe the transition between  $P_1$  and  $P_2$  in  $P_2 \circ P_1$  is a product output. Thus, all of the edges of  $P_1$  must be labeled before any edge in  $P_2$  is labeled. Furthermore, the terminal product output edge of  $P_1$  becomes the 1-valent root edge of  $P_2$ , which would not have appeared in  $T_2$ , so no additional entries are added to  $\phi(P_2 \circ P_1)$  that are not in  $T_1$  or  $T_2$ . Thus,  $\phi(P_2 \circ P_1)$  will contain  $T_1$  in the first  $n_1$  columns and a scaled-up  $T_2$  in the final  $n_2$  columns.  $\square$

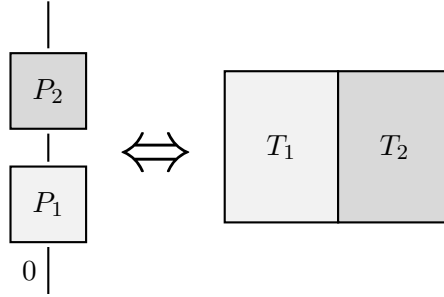


Figure 14: Composition operation  $P_2 \circ P_1$  and associated tableau  $\phi(P_2 \circ P_1)$

### 4.3 Closed Product

The final operation we investigate is the closed product of  $k$   $k$ -ary prographs. The **closed product** of  $k$   $k$ -ary prographs, where  $P_i \in PC^k(n_i)$ , is denoted  $P^* = P_1 * \dots * P_k$  and lies in  $PC^k(n_1 + \dots + n_k + 1)$ . The closed product  $P^*$  joins these  $k$  prographs at the bottom by a  $k$ -ary coproduct and at the top by a  $k$ -ary product. See Figure 15 for an example of  $P^*$  and how the constituent tableaux appear within  $\phi(P^*)$  for three 3-ary prographs  $P_1, P_2, P_3$ . Moreover, Theorem 4.3 describes this relationship in detail.

**Theorem 4.3.** *Take  $P_1, \dots, P_k$ , where  $P_i \in PC^k(n_i)$ , and let  $T_i = \phi(P_i)$ . Then,  $\phi(P^*) \in \mathbb{S}(\lambda, \rho)$  with  $\lambda = (1 + \sum_1^k n_i, 1 + \sum_1^k n_i, 1 + \sum_1^k n_i)$  and  $\rho = (1, k - 1, 1)$ . The individual tableaux  $T_1, \dots, T_k$  will appear within  $\phi(P^*)$  as scaled-up, skew tableaux, given below.*

- $T_1$  within  $\phi(P^*)$  has shape  $\lambda_1 = (n_1 + 1, n_1, n_1)$  minus  $\mu_1 = (1, 0, 0)$  and density  $\rho_1 = (1, k - 1, 1)$ .
- For  $1 < i < k$ ,  $T_i$  within  $\phi(P^*)$  has shape  $\lambda_i = (n_i + 1, n_i + 1, n_i)$  minus  $\mu_i = (1, 0, 0)$ , and density  $\rho_i = (1, (k - i, k - 1, \dots, i - 1), 1)$ .
- $T_k$  within  $\phi(P^*)$  has shape  $\lambda_k = (n_k + 1, n_k + 1, n_k)$  minus  $\mu_k = (1, 1, 0)$  and density  $\rho_k = (1, k - 1, 1)$ .



*Proof.* Within  $P^*$ , the bottom coproduct outputs correspond to the initial input edges of the individual prographs  $P_1, \dots, P_k$ , which would normally be labeled as 0. The bottom coproduct connects these graphs with a new input edge, which is now labeled 0. The shift of 1 in the top row of  $T_1$  is due to the initial input of  $P_1$  labeled 1, shown in Figure 15.

The initial input edges of prographs  $P_i$  for  $1 < i < k$  become non-left coproduct edge in the product, and those labels will appear in the middle row. In the overall tableau, these initial input labels will separate  $T_i$  from  $T_{i+1}$ . To remove these extra integers from the middle row of  $T_i$ , the far-left box will receive  $k - i$  integers from  $P_i$ , and the far-right box will receive  $i - 1$  integers from  $P_i$ . The left and right arrows in Figure 15 correspond to the separation of these extra integers from either side of  $T_i$ .

After prograph  $P_{k-1}$ , the far-right middle box in  $T_{k-1}$  will have  $k - 2$  integers, and then the initial input edge of  $P_k$  will be added to this box. Therefore,  $T_k$  will again have constant density across the middle row. The initial skew of the top row of  $T_1$  skews the top row of every  $T_i$ , as seen in Figure 15. The extra  $k - 1$  integers in the middle row cause the middle row of  $T_k$  to be skewed by one box. The uncolored box in Figure 15 at the bottom-right corner corresponds to the final product output.  $\square$

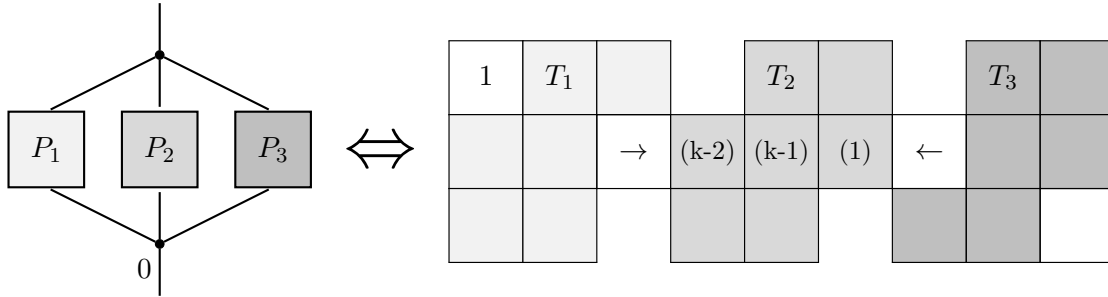


Figure 15: Closed product  $P_1 * P_2 * P_3$  and associated tableaux  $\phi(P^*)$

In Figure 15, the middle boxes in  $\phi(P^*)$  which separate  $T_1$  from  $T_2$  and  $T_2$  from  $T_3$  will contain integers from  $\phi(P_2)$  alongside the integers corresponding to the newly-labeled input edges. Therefore, we have placed the two arrows to denote the separation of these elements from  $T_2$ . By considering these three operations, we were able to explore the depths of our bijection and how certain constructions of tableaux and prographs influence the other.

## 5 Limited Explorations

We conclude with a proposition and theorem that we investigated yet fell outside the general flow of this paper. First, we consider closed prographs such that each coproduct has  $k$  outputs and each product has only  $k - 1$  inputs. We denote the set of these prographs as  $PC^{k,k-1}(n)$ . In order for these these prographs be closed, the extra coproduct edges need to be trapped within a product, as shown in Figure 16.

We give a possible formula to enumerate prographs of this type when  $n = 2$ , stated in Conjecture 5.1. We do not consider this a major result because we could not find a bijection between prographs of this type and standard set-valued tableaux.



Figure 16: Example of a prograph in  $PC^{3,2}(2)$

**Conjecture 5.1.** *For closed prographs with  $n = 2$ ,  $k$  coproduct outputs, and  $k - 1$  product inputs,  $PC^{k,k-1}(2) = 3k^2 + 6$ .*

Next, we examine a theorem we develop to count  $k$ -ary prographs such that the top of the prograph is justified. This means the rightmost input of all products is the output of the previous product. The standard set-valued tableaux that correspond to these prographs behave in such a way that if the bottom row of the tableau was removed, this would result in a two row standard set-valued tableau.

**Theorem 5.2.** *For any  $n \geq 1$  and  $k \geq 1$ , the number of prographs such that all product children are labeled last in the left-ascending search is  $C_n^k$ .*

*Proof.* Since all of the products are numbered last, we know that the bottom row will have the largest integers in the corresponding tableau. So removal of the bottom row will in this specific case will not change the number of potential tableaux. Thus, we have a direct bijection between these prographs and standard set-valued tableaux of shape  $\lambda = (n, n)$  and density  $\rho = (1, k - 1)$ . Note, you could perform the Schützenberger involution on these tableaux, and then you would get two row standard set-valued tableaux of density  $\rho = (k - 1, 1)$ . Which we already know these tableaux are counted by the  $k$ -Catalan numbers,  $C_n^k$  □

Thus, Theorem 5.2 gives a direct bijection between certain three row standard set-valued tableaux and two row standard set-valued tableaux, considered by Heubach, Li, and Mansour [3]. Since this connection is rather limited, we consider this a minor result. Although these have not been particularly fruitful avenues within our research, future mathematicians may find more useful applications of these concepts.

## 6 Open Questions for Future Work

Below are some possible directions for future research:

- Although we have counted standard set-valued tableaux for a few particular shapes, we have not yet found a closed-formula for arbitrary shape and density. Enumerating standard set-valued tableaux of shape  $\lambda = (n, n, n)$  and density  $\rho = (1, k - 1, 1)$  may be accomplished by finding a closed formula for  $PC^k(n)$  for any  $n \geq 1$ ,  $k \geq 1$ , which we believe may be a tractable method.
- It is likely possible to generalize our bijection for non-closed prographs where  $x \not\equiv 1 \pmod{k - 1}$ . Intuitively, we predict these  $k$ -ary prographs will map to standard set-valued tableaux with non-row-constant densities.

- We also hope a combinatorial representation for set-valued Young tableaux with density  $\rho = (1, 1, k-1)$  will be found. More generally, future research could concern other combinatorial objects that relate to standard set-valued tableaux of various three row shapes and densities.
- Related to the previous note, we considered extending a bijection between standard Young tableaux and Motzkin Paths found by Eu [6]. Their result equates the number of Motzkin paths of length  $n$  and the number of standard  $n$ -cell Young tableaux of at most three rows. We thought of extending this result to include  $k$ -Motzkin paths of length  $n$  and standard set-valued  $n$ -cell tableaux of at most three rows and density  $\rho = (1, k-1, 1)$ . By  $k$ -Motzkin paths of length  $n$ , we mean lattice paths from  $(0, 0)$  to  $(n, 0)$  that use steps  $(1, k-1)$ ,  $(1, 0)$ , and  $(1, -1)$  and which never fall below the line  $y = 0$ .

## 7 Acknowledgements

This research would not have been possible without funding from the National Science Foundation, grant DMS-1559912. Furthermore, we extend our sincerest gratitude to the Valparaiso Experience in Research by Undergraduate Mathematicians program for providing us with the opportunity to conduct this research, Valparaiso University for hosting us, and our mentor, Dr. Paul Drube, for advising us during this project. Finally, we'd like to thank Benjamin Levandowski from Valparaiso University for providing us with his Java code.

## References

- [1] J Sutherland Frame, G de B Robinson, Robert M Thrall, et al. The hook graphs of the symmetric group. *Canad. J. Math*, 6(316):C324, 1954.
- [2] William Fulton. *Young tableaux: with applications to representation theory and geometry*, volume 35. Cambridge University Press, 1997.
- [3] Silvia Heubach, Nelson Y Li, and Toufik Mansour. Staircase tilings and k-catalan structures. *Discrete Mathematics*, 308(24):5954–5964, 2008.
- [4] Paul Drube. Set-valued tableaux & generalized catalan numbers. *arXiv preprint arXiv:1607.07411*, 2016.
- [5] Nicolas Borie. Three-dimensional catalan numbers and product-coproduct prographs. *arXiv preprint arXiv:1704.00212*, 2017.
- [6] Sen-Peng Eu. Skew-standard tableaux with three rows. *Advances in Applied Mathematics*, 45(4):463–469, 2010.